The Effect of the 1997/98 El Niño on Individual Large-Scale Weather Events

Joseph J. Barsugli,* Jeffrey S. Whitaker,* Andrew F. Loughe,*
Prashant D. Sardeshmukh,* and Zoltan Toth+

ABSTRACT

Can an individual weather event be attributed to El Niño? This question is addressed quantitatively using ensembles of medium-range weather forecasts made with and without tropical sea surface temperature anomalies. The National Centers for Environmental Prediction (NCEP) operational medium-range forecast model is used. It is found that anomalous tropical forcing affects forecast skill in midlatitudes as early as the fifth day of the forecast. The effect of the anomalous sea surface temperatures in the medium range is defined as the *synoptic El Niño signal.* The synoptic El Niño signal over North America is found to vary from case to case and sometimes can depart dramatically from the pattern classically associated with El Niño. This method of parallel ensembles of medium-range forecasts provides information about the changing impacts of El Niño on timescales of a week or two that is not available from conventional seasonal forecasts.

Knowledge of the synoptic El Niño signal can be used to attribute aspects of individual weather events to El Niño. Three large-scale weather events are discussed in detail: the January 1998 ice storm in the northeastern United States and southeastern Canada, the February 1998 rains in central and southern California, and the October 1997 blizzard in Colorado. Substantial impacts of El Niño are demonstrated in the first two cases. The third case is inconclusive.

1. Introduction

During the 1997/98 El Niño all sorts of severe weather events in the extratropics, from snowstorms, ice storms, and flooding to tornado outbreaks and droughts, were attributed to El Niño. "Blame it on El Niño" was a recurrent theme in both the popular media and in statements by atmospheric scientists. Others argued on statistical grounds that only the cumulative influence of El Niño over a season is detectable, not its influence on individual storms. Now that this warm event has drawn to a close and regional assessments of the impacts of El Niño are being made, it is important to bring to bear as much scientific evidence as possible on whether such attribution is warranted. More importantly, scientific diagnosis of the mechanisms by which tropical SST anomalies influence the midlatitudes on subseasonal timescales will provide a more detailed understanding of the global effects of El Niño.

We address the question, Can individual, large-scale weather events during the 1997/98 winter be attributed to El Niño? We introduce a new method to accomplish this. In a nutshell, ensemble forecasts using the National Centers for Environmental Prediction (NCEP) Medium-Range Forecast (MRF) model were run with climatological sea surface temperatures (SSTs) in the Tropics. These runs were compared with NCEP's operational MRF ensembles run with the observed El Niño SST anomalies, starting from the same initial conditions. Differences between the two sets of runs manifest themselves globally within 5 days and become substantial in the second week of the forecast. We call this difference the "synoptic El Niño signal." We find that the synoptic El Niño signal varies from week to week and involves mechanisms of interaction between the Tropics and extratropics that have received little attention in the meteorological literature.

*NOAA–CIRES Climate Diagnostics Center, Boulder, Colorado.
+NOAA/NCEP/EMC, Washington, D.C.
Corresponding author address: Dr. Joseph J. Barsugli, CIRES, Campus Box 216, University of Colorado, Boulder, CO 80309.
E-mail: jjb@cdc.noaa.gov
In final form 8 April 1999.

Our method provides more information than conventional seasonal forecasts based on long-term observed correlations or based on simulations with climate general circulation models, because it can detect nonstandard or "unexpected" effects of El Niño. Because our method is based on forecasts made with a skillful weather prediction model with observed initial conditions, we can also make deductions about individual weather events that occurred in nature. The statistics generated by the ensemble forecasting method enable statistical testing of the robustness of our conclusions. There is, however, one major limitation to our study that is inherent in our use of forecasts made with observed initial conditions: we are only able to deduce the cumulative effects of El Niño *during the forecast period.* The effects of El Niño on the initial conditions themselves are not accounted for. Therefore our method probably provides a conservative assessment of the effects of El Niño.

2. Method of parallel ensembles

Every day an ensemble of 11 forecasts starting from 0000 UTC initial conditions is run at NCEP using a 28-level version of the MRF model spectrally truncated to 62 waves [see Toth and Kalnay (1997) for a primer on ensemble forecasting at NCEP and Kanamitsu et al. (1991) for a description of the MRF model]. These forecasts are run out to 16 days. A smaller ensemble is also run with 1200 UTC initial conditions, but it is not used in this study. The initial conditions are generated using the "breeding" technique described in Toth and Kalnay (1993). The initial conditions are centered on the operational analysis, and their spread is intended to be representative of the analysis error.

At the Climate Diagnostics Center (CDC) we ran the 0000 UTC ensemble out to 14 days, specifying climatological SSTs in the Tropics. The initial conditions and all other boundary conditions for the ensembles at NCEP and CDC were identical. We refer to the climatological SST runs as the CLIMOSST ensemble and to the operational runs as the NINOSST ensemble. The CLIMOSST ensembles were run starting every other day for the period from 1 December 1997 to 31 March 1998. After mid-January the integrations were done in near–real time, and the results were graphically displayed on the CDC Web site (http://www.cdc.noaa.gov). We also performed special integrations to look at other cases such as the October 1997 blizzard in Colorado discussed later in this paper.

The SST boundary conditions for the CLIMOSST runs at CDC were constructed as follows: equatorward of 20° latitude climatological SSTs were used; poleward of 30° latitude in both hemispheres the operational SST analysis was used; and between 20° and 30° latitude the operational and climatological SST fields were linearly blended. The SSTs were held fixed during both the NINOSST and CLIMOSST forecasts. The SST climatology was defined as the 1982–96 average of the daily SST values from the NCEP reanalysis dataset (Kalnay et al. 1996). The particular averaging period was chosen so that the SST analysis scheme used in determining our climatology would be consistent with that used for the current operational SST analysis.

Three quantities of central importance to this study are ensemble spread, synoptic El Niño signal, and forecast skill. The *ensemble spread* is defined as the standard deviation of the ensemble members about the ensemble mean. Ensemble spread gives an estimate of the uncertainty of the forecast. The *synoptic El Niño signal,* or simply *signal* is defined as the difference between the NINOSST ensemble mean and the CLIMOSST ensemble mean. Both spread and signal are defined for all forecast lead times at all geographical locations. We measure *forecast skill* in two ways: root-mean-square (rms) error and anomaly correlation (AC). Rms error is defined as the root-mean-square difference between the forecast and the verification, where the area-weighted mean is taken over all grid points in a specified geographical region. The anomaly correlation is the area-weighted spatial correlation coefficient in some specified geographical region between the ensemble mean forecast and the verification, where the long-term climatological mean from observations (NCEP reanalysis, 1968–96) is removed from both fields. The spatial mean is not removed when computing the spatial correlation. For example, if both forecast and verification contain a positive anomaly with respect to the climatology over the entire region, we credit some skill to the model. All verification fields are from the NCEP reanalysis (Kalnay et al. 1996). The term "forecast" used without qualification refers to the mean of the ensemble members. In calculating the skill of time-averaged forecasts, such as the 6–10-day forecast, the time averaging of the forecasts and verifications are performed prior to the calculation of skill.

The statistical significance of the synoptic El Niño signal at a given location was tested by comparing the magnitude of the signal to the value of the ensemble spread, scaled by the square root of the size of the en-

semble. For all variables except precipitation Student's t-statistic was used to determine one-sided 95% confidence levels that the signal differs from zero. For precipitation, the 95% confidence level was determined via a Monte Carlo technique where the two ensembles were pooled and randomly resampled with replacement. Pairwise differences of sample means were ranked, determining the 5th and 95th percentiles. These significance tests address the reproducibility of the signal if we had repeated these experiments with a different set of initial conditions generated using the same procedure. In this test we do not take into account that the same set of initial conditions is used in each ensemble (i.e., that the runs are paired). Extrapolating from the significance test *with respect to the ensemble spread* to statements *with respect to the real atmosphere* depends on the extent to which ensemble spread reflects forecast error. Since the rms forecast error is typically greater than ensemble spread, the significance test is probably somewhat lenient.

Rapid adjustment of the tropical precipitation field (and hence the divergent circulation) to the underlying SSTs is necessary for the success of this experiment. The development of the El Niño signal in tropical precipitation) 20°N–20°S average) is shown in Fig. 1a. Substantial adjustment to the climatological SSTs occurs within the first 24 h of the forecast, and the adjustment is nearly complete by 48 h. The average tropical precipitation signal for week 2 of the forecast (Fig. 1b) compares well with the NCEP reanalysis precipitation anomaly (not shown) and an independent satellite microwave estimate of precipitation [Fig. 1c, modified Hughes D-matrix algorithm; Berg et al. (1998)]. It should be noted that both the NINOSST (operational) and CLIMOSST runs undergo an additional adjustment in the tropical precipitation field due to imbalances in the initial conditions introduced by the data assimilation procedure. This adjustment is also very rapid, with most of the adjustment in the NINOSST total precipitation occurring in the first 12–24 h of the forecast (not shown). Because the assimilation-induced condition imbalances are identical in both sets of runs, the effects should tend to cancel out when computing the El Niño signal. Nevertheless, transient adjustment should be taken into account when interpreting the El Niño signal during the early part of the forecast period.

While this study is mainly concerned with the case-to-case variations in the signal, it is instructive first to consider the mean over all cases of the 500-mb signal (Fig. 2). The mean signal shows the development of a wave train that propagates out of the Tropics. By day 10 the mean signal resembles the observed seasonal mean anomaly for the past winter (December–March). This signal is consistent with the wintertime El Niño signal seen in historical observations (e.g., Horel and Wallace 1981; Livezey et al. 1997) and in 1997–98 wintertime seasonal forecasts. The cases discussed in section 3 demonstrate that the synoptic El Niño signal can depart considerably from the seasonal mean signal.

3. Case studies

We have chosen three cases—one unusual, one canonical, and one inconclusive—to illustrate how our

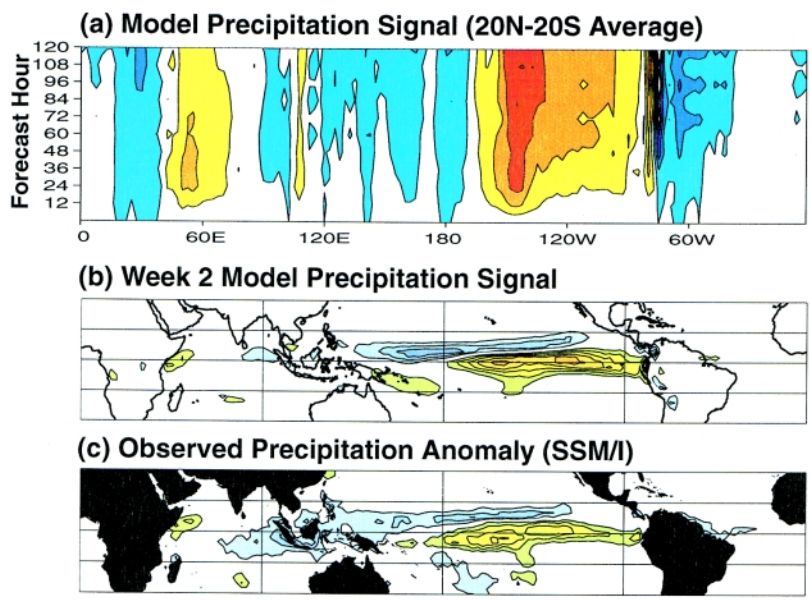

FIG. 1. (a) Tropical precipitation signal averaged over all cases for Dec–Jan–Feb–March (DJFM) 1997–98 and averaged over latitudes 20°N–20°S, as a function of longitude and forecast lead time. The accumulated precipitation over the 12 h prior to the nominal time is contoured (contour interval 1 mm day^{-1}; blue shading is negative). (b) Week 2 mean precipitation signal (contour interval 3 mm day^{-1}; zero contour suppressed) for the same period. (c) Satellite [Special Sensor Microwave/Imager (SSM/I)] estimate of DJFM 1997–98 precipitation [same units as in (b)] anomaly from 1988–96 climatology.

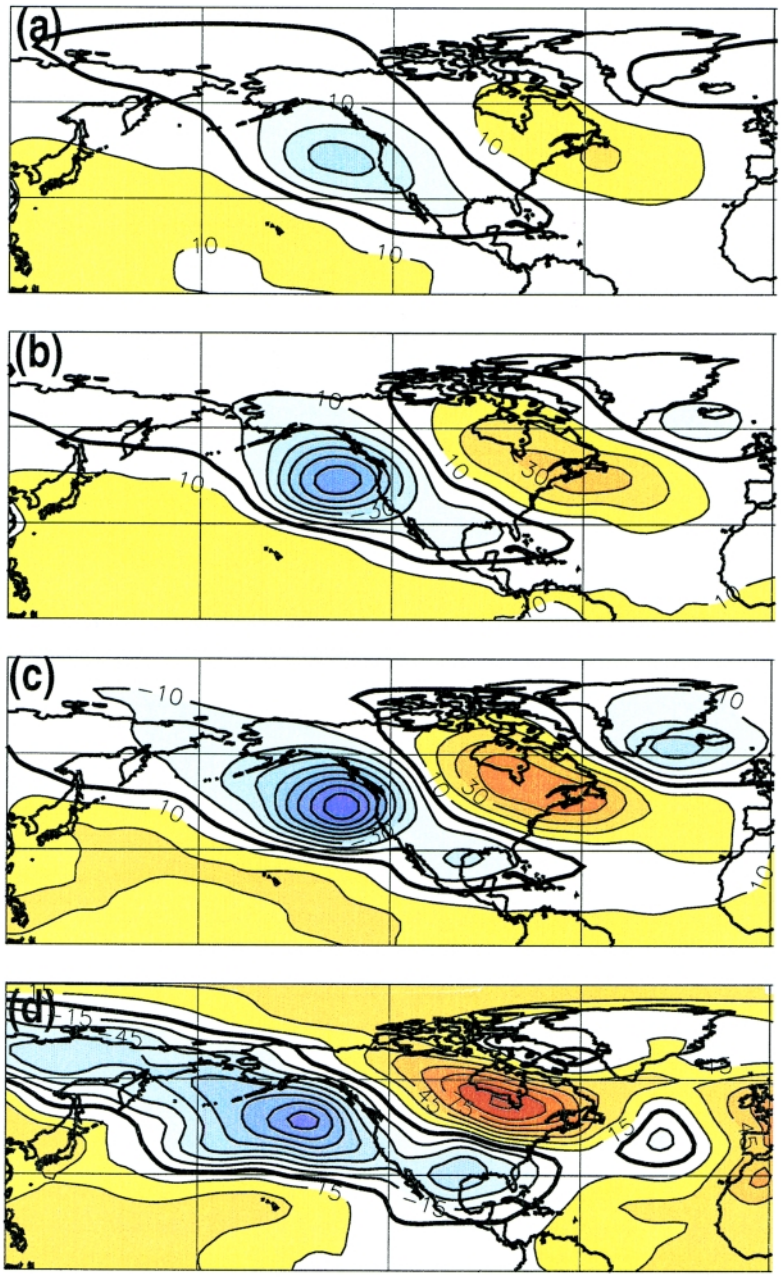

FIG. 2. Mean 500-mb height signal over all 61 cases from 1 Dec 1997–31 Mar 1998 for (a) 7-day forecasts, (b) 9-day forecasts, and (d) 11-day forecasts. The mean observed 500-mb height anomaly for the same period is shown in (d). Contour interval is 10 m for (a)–(c), 15 m for (d). The zero line is the thicker contour.

method can be used to detect the effects of El Niño on individual weather events.

a. Ice storm: 5–10 January 1998

Perhaps the most striking and provocative result of this study involves the devastating ice storm that hit southeastern Canada and the northeastern United States in early January 1998. As much as 10 cm of ice accumulated in certain locales, causing widespread power outages, disruption to travel and commerce, and loss of life. According to Environment Canada, this ice storm was "by far the costliest weather catastrophe in Canadian history" (Francis and Hengeveld 1998). Heavy damage also occurred in the United States. Ice storms in this area are common, but this storm was very unusual in its duration, spatial extent, and in the amount of ice that accumulated (Higuchi et al. 1999, manuscript submitted to *Mon. Wea. Rev.*). We are not aware of any research pointing to a statistical connection between El Niño and ice storms in this area. Nevertheless, aspects of this storm can be attributed to El Niño.

The observed large-scale flow pattern at the time of the storm (Fig. 3d) was dominated by an anomalous anticyclone centered over the Maritime provinces with associated warm temperatures at midlevels. A surface warm front extended across northern New England and southern Quebec (not shown). Low-level anomalous southeasterlies brought large quantities of warm moist air at midlevels over the hard-hit areas. In fact, the warm advection was so unusual that it led to record high temperatures along the mid-Atlantic coast as well. North of the frontal boundary a significant amount of precipitation was in the form of freezing rain. That the precipitation fell as freezing rain rather than snow was largely due to the midlevel warmth. We will focus on this 500-mb circulation feature as an essential factor in the development of the ice storm. A more detailed synoptic analysis of the ice storm can be found in Higuchi (1999, manuscript submitted to *Mon. Wea. Rev.*).

What produced this circulation feature? In Fig. 3 we compare the 6–10-day mean forecasts of the 500-mb height anomaly from the NINOSST and CLIMOSST forecasts begun on 1 January 1998. The synoptic El Niño signal for this case along with the corresponding observed 5-day mean 500-mb height anomaly are also shown. The rms error in the sector shown is reduced from 93 to 69 m by the inclusion of

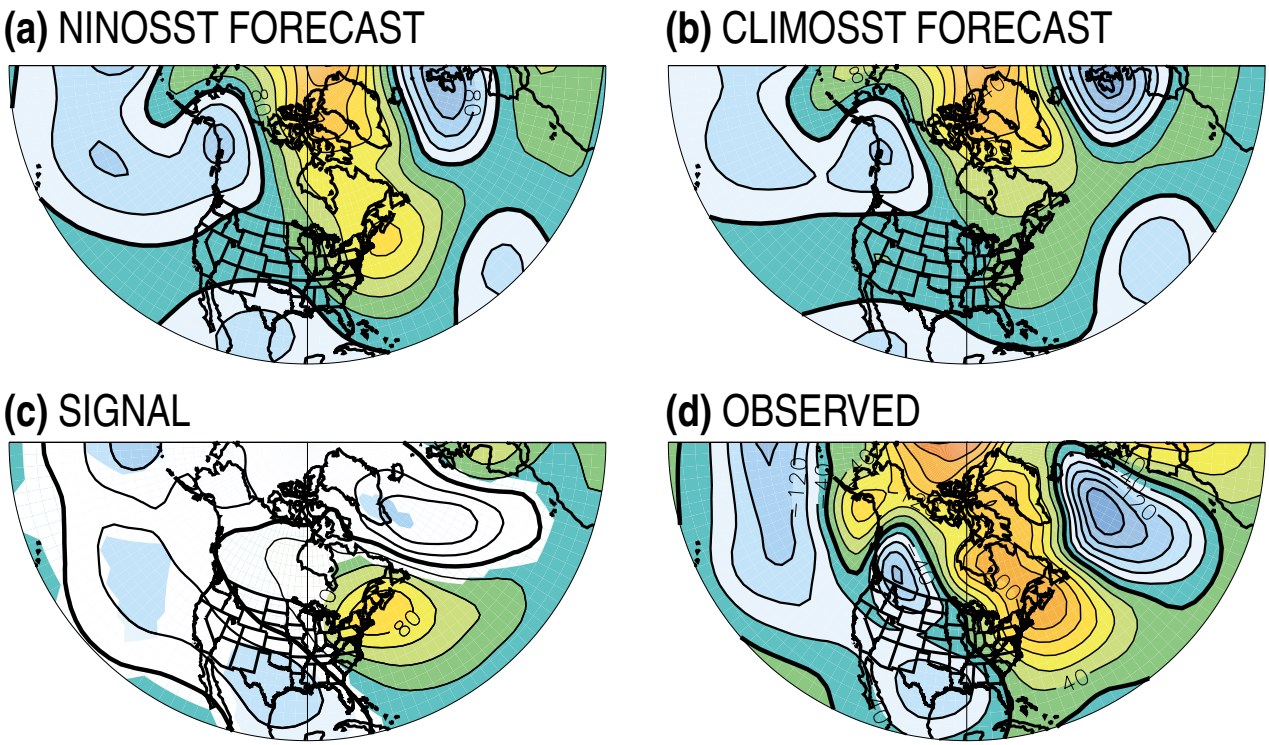

FIG. 3. The 6–10-day mean forecasts of 500-mb height anomaly initialized on 1 Jan 1998 for the "ice storm" case: (a) NINOSST forecast, (b) CLIMOSST forecast, (c) the synoptic El Niño signal. In (c), the regions that are not color-filled are not statistically significant using the test described in section 2. The observed 500-mb height anomaly corresponding to the forecast period is shown in (d). Contour interval is 40 m in (a) and (b), and 20 m in (d). The zero line is the thicker contour.

the anomalous tropical SSTs in the forecast. Because the anomalous high and associated flow pattern was well forecast in days 6–10 in the NINOSST ensemble, and because the CLIMOSST runs did not produce this feature, we conclude that El Niño had a strong impact on the location and severity of the ice storm.

The synoptic El Niño signal in 500-mb height (Fig. 3) shows what appears to be a wave train oriented along the Atlantic coast of North America. We speculate that this "Atlantic coast wave train" is the signature of a Rossby wave forced by anomalous tropical convection associated with El Niño. This wave train differs from the canonical seasonal mean response to El Niño discussed above. We hypothesize that the unusual trajectory followed by this wave train may have resulted from Rossby wave ducting by the unusually deep 500-mb trough that was present over North America in early January 1998, or from anomalous Rossby wave sources due to the interaction of this trough with tropical convection in the eastern Pacific. Further diagnosis of Rossby wave propagation on time-varying base states and of anomalous Rossby wave sources is under way using a linearized version of the model dynamics.

Undoubtedly, many other meteorological factors contributed to the development of the ice storm, including a strong low-level inversion with subfreezing temperatures near the surface and the associated surface front. Though we have not assessed the effect of El Niño on these factors, we speculate that the MRF model may not simulate the intensity or location of these sharp features as well as it does the large-scale 500-mb flow at a lead time of one week. This complex interplay of factors underscores the need for informed interpretation of the results presented here. Also, we have only diagnosed the effect of El Niño forcing during the week before the ice storm; we cannot ascertain the effect of El Niño prior to the initialization of the forecasts on 1 January. Nevertheless, this case demonstrates the usefulness of our method in detecting and understanding some unusual and unexpected effects of El Niño.

b. California rains: 1–14 February 1998

In February 1998 central California received large amounts of rainfall resulting in widespread flood damage and several deaths. Based on traditional seasonal forecasts, increased wintertime California rainfall was one of the most widely anticipated effects of El Niño.

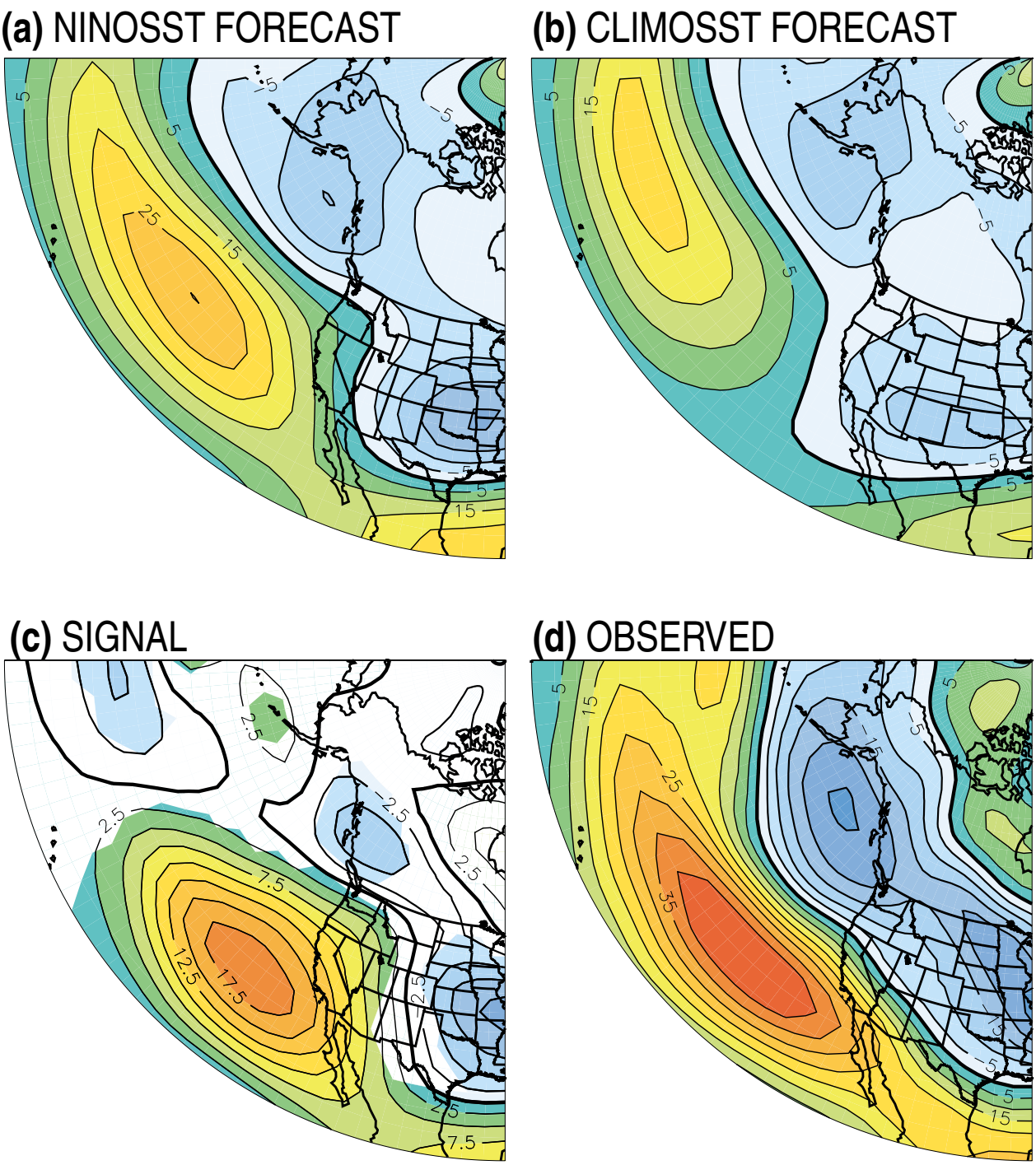

FIG. 4. The 8–14-day mean forecasts of 250-mb zonal wind anomaly initialized on 24 Jan 1998 and verifying the first week of February 1998 (the "California rain" case): (a) NINOSST forecast, (b) CLIMOSST forecast, (c) synoptic El Niño signal. In (c), the regions that are color-filled are statistically significant using the test described in section 2. The observed 250-mb zonal wind anomaly corresponding to the forecast period is shown in (d). Contour interval is 5 m s^{-1} in (a), (b), and (d), and 2.5 m s^{-1} in (c). The zero line is the thicker contour.

Although it was feared that the rains would start as early as December, the onset of the heavy rains did not occur until mid-January, with the heaviest rains occurring during February.

Initially we will focus on the rain that fell during the first week of February. This "event" involved the cumulative effect of several synoptic-scale storms, the eastward extension of the jet stream, and a strength-

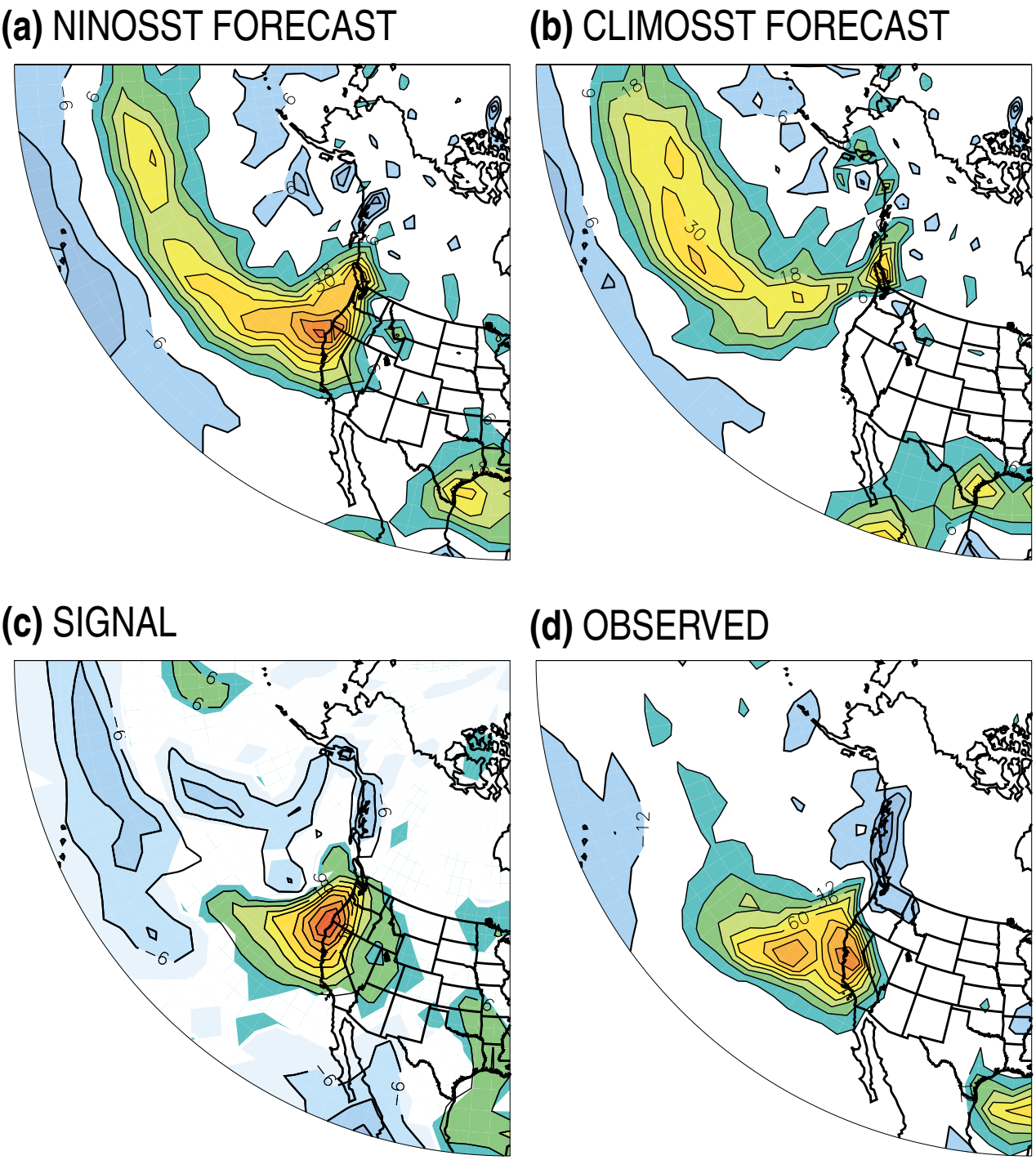

FIG. 5. As in Fig. 4 except for accumulated precipitation. Contour interval is 6 mm for (a)–(c) and 12 mm for (d), the observed precipitation (estimated from the NCEP reanalysis). Statistically significant regions are shaded in (c). The zero line is omitted for clarity.

ening and eastward shift of the Aleutian low. What was the effect of El Niño during this period? In Fig. 4 we compare the 8–14-day mean forecasts of 250-mb zonal wind anomaly from the NINOSST and CLIMOSST forecasts begun on 30 January 1998. The synoptic El Niño signal and the corresponding observed 7-day mean anomaly are also shown. The rms error in the sector shown is reduced from 14 to 10 m s^{-1} by the inclusion of the anomalous tropical SSTs during the forecast. The reduction in error is particularly evident

in the vicinity of the jet stream offshore from California, where the El Niño signal is strong. A more dramatic picture is shown in Fig. 5, which depicts the same comparison for precipitation. As in the ice storm case discussed above, the NINOSST forecast was much closer to the verification than was the CLIMOSST forecast, and the El Niño signal was a prominent feature of the observed event. Our method clearly attributes a sizable portion of the rainfall in central California during this period to El Niño.

Over the entire 1997/98 winter the synoptic El Niño signal in precipitation broadly coincides with the actual subseasonal variation in regional rainfall anomalies in central California (Fig. 6). We conclude that a sizable portion of the anomalous rainfall in this region in February can be attributed to El Niño on a week-by-week basis. In contrast, the rainy period in early January coincides with a period of little or no synoptic El Niño signal, with the NINOSST and CLIMOSST runs producing roughly the same amount of rain. We conclude that *by our measure* there was a negligible impact of El Niño in central California during this earlier period. As noted above, we cannot rule out possible impacts of El Niño on these rains through its impact on the initial conditions.

Finally, we note that in the vicinity of California certain aspects of the response El Niño are felt with surprising rapidity. For example, the 72-h forecast begun on 1 February 1998 has an El Niño signal in 250-mb zonal winds of 8 m s^{-1} off the coast of California (not shown). These anomalous winds may be attributed to an anomalous local Hadley cell forced by the tropical convection that is present in the NINOSST runs and absent in the CLIMOSST runs. There are numerous other examples of similarly rapid communication between the Tropics and the subtropical jet in this region. We presume that subseasonal variations in tropical convection during an El Nino winter, such as those associated with the Madden–Julian oscillation, may be felt equally quickly in this region. This would imply that improving the forecasts of subseasonal variations in large-scale tropical convection would improve forecast skill in the subtropics and over California. In summary, our method can attribute to El Niño some portion of the canonical enhancement of wintertime California rainfall to El Niño on roughly a week-by-week basis, though some question remains as to how fine a temporal resolution is really possible.

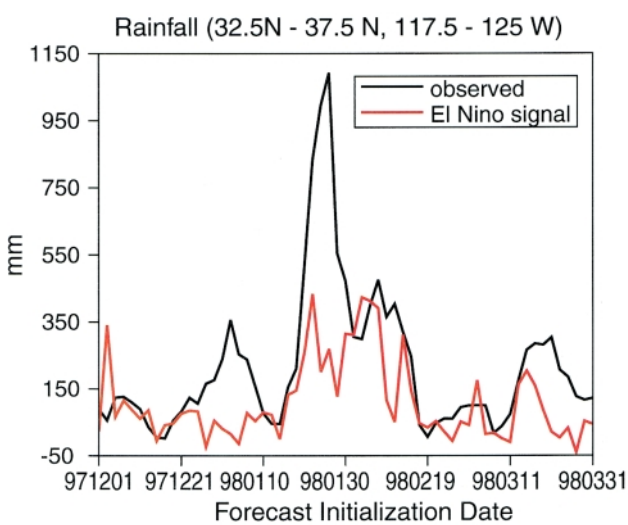

FIG. 6. Central California precipitation (integrated over the region indicated) from 1 Dec 1997 to 31 Mar 1998. Black curve is observed weekly precipitation and red curve is El Niño precipitation signal from the 8–14-day forecasts.

c. Colorado blizzard: 25 October 1997

On 25 October 1997 a blizzard struck Colorado and the Great Plains. Among the impacts, the storm stranded hundreds of travelers at Denver International Airport for up to 3 days. The *Denver Post* headlines read "El Niño's First Punch," while the *Rocky Mountain News* announced "El Niño Not to Blame for Storm." Could our method resolve this dilemma by finding evidence of a significant El Niño connection? (Recall that our method cannot strictly rule out all effects of El Niño, only those during the forecast period.) We ran both NINOSST and CLIMOSST ensembles at CDC for the forecast beginning on 16 October 1997. Figure 7 shows the 500-mb signal at day 10. The signal is extremely weak. The extratropical signal at other forecast lead times and for other variables is similarly weak. The reason for this is ultimately rooted in the Tropics, where the precipitation signal is extremely weak during the first 5 days of the forecast and remains weak until day 10. Since tropical convection is a necessary (but not sufficient) part of the mechanism by which tropical–extratropical teleconnections are produced, one would expect little 500-mb signal in the midlatitudes.

To what extent is the model's weak tropical precipitation signal believable, given the large observed SST anomalies? The left panels of Fig. 8 show the total NINOSST precipitation for days 0–4 and days 5–9 of the forecast. The right panels show the actual pentad precipitation as estimated from satellite microwave measurements (Berg et al. 1998). The convection in the model is much too weak during the initial period over the tropical Pacific, particularly near the

date line. When the anomalous SSTs are "turned off," there is little change in the model's convection where there was little convection to begin with. In days 5–9 the model fails to capture the "flare-up" of convection that occurred just south of the equator and east of the date line. While inconclusive about the effects of El Niño over Colorado in this case, our results point to a model deficiency in the initialization and simulation of tropical precipitation in this case. Note that tropical precipitation was qualitatively better simulated for most of the other cases in this study (as shown in Fig. 1). Nevertheless, addressing deficiencies in the prediction of large-scale tropical precipitation should be a high priority since our study demonstrates the potential for the first week of the tropical forecast to affect the second week of the midlatitude forecast (see also Ferranti et al. 1990).

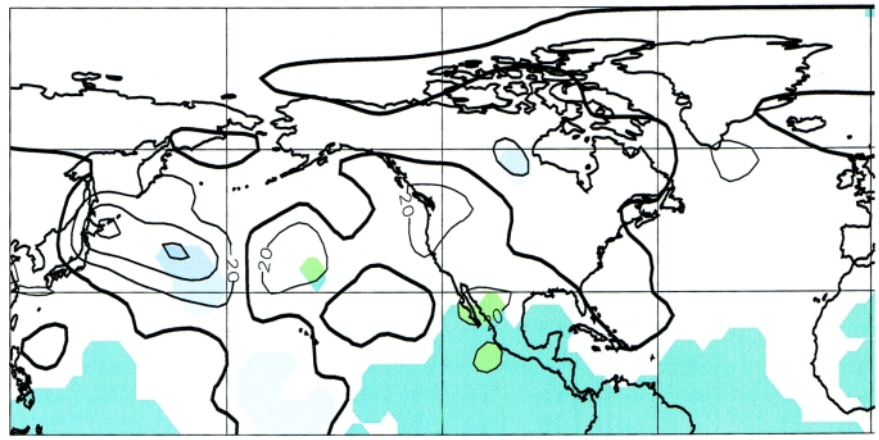

FIG. 7. Day 10 El Niño signal in 500-mb height for the "Colorado snowstorm" case initialized on 16 Oct 1998. Contour interval is 20 m, zero line is thicker, color-filled regions are statistically significant according to the test described in section 2.

In summary, when we apply our method to the 25 October case, it unfortunately proves inconclusive on the question of attribution. However, even if the model had produced a better simulation of tropical convection, there is no guarantee it would have produced a large signal in midlatitudes. This case illustrates some of the drawbacks of this method, but also demonstrates the usefulness of these runs in helping diagnose errors in model physics even when attribution is inconclusive.

4. Discussion

a. *Conceptual framework*

In Fig. 9 we present a simple schematic figure that

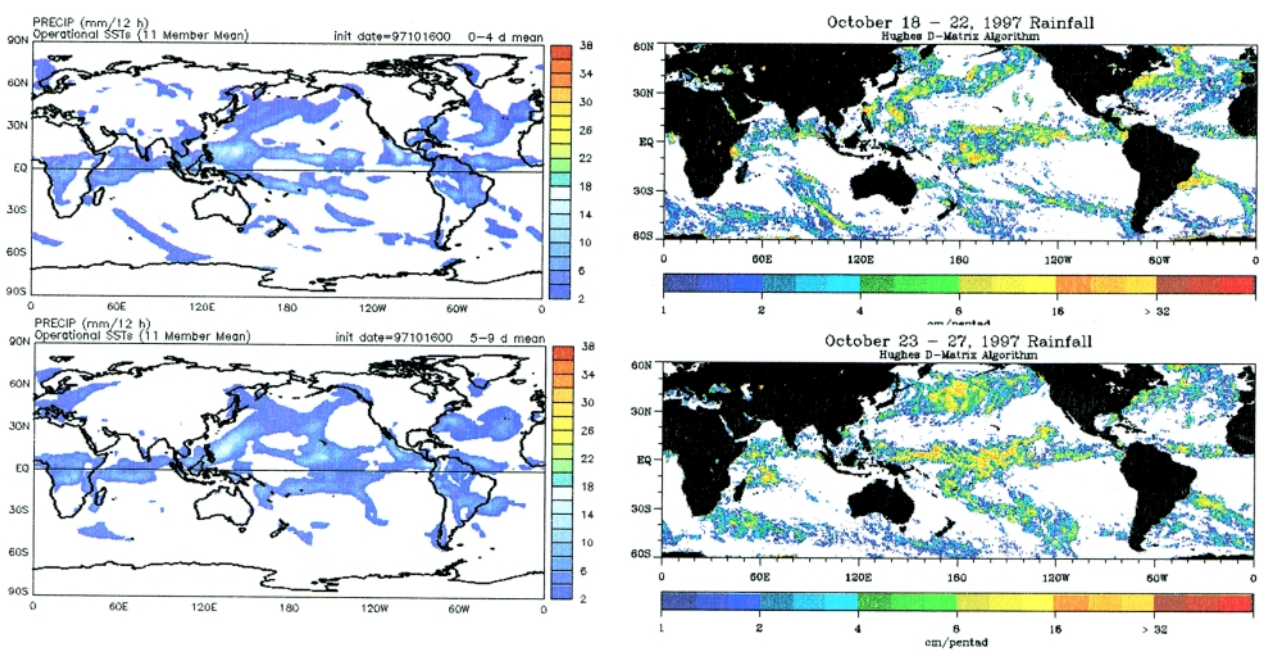

FIG. 8. Left panels show the total ensemble mean precipitation from the NINOSST forecast averaged over the first 5 and the second 5 days of the forecast. Right panels show the satellite (SSM/I) estimated rainfall for the nearest available pentads.

illustrates how our method fits in to a larger framework that encompasses traditional seasonal forecasting and ensemble weather forecasting. To simplify the discussion in this section we use the normal (Gaussian) probability distribution whose probability density function (PDF) is the familiar "bell curve." With minor modifications, the arguments given below apply for more general probability distributions. We also ignore the effects of model systematic error in this discussion.

The traditional seasonal forecasting problem for wintertime North America largely boils down to predicting the expectation values of such variables as temperature and precipitation given tropical SST anomalies (either persisted or forecast). The black curves in Fig. 9d show a schematic PDF for some atmospheric variable assuming tropical SSTs are near normal. The red curves in Fig. 9d show the conditional distribution of the same variable given that an El Niño of a given amplitude occurs. For concreteness, consider these curves to be histograms of daily temperature at some location during "normal SST" and "El Niño" years, respectively. At this hypothetical location, temperatures are on average warmer in an El Niño year than otherwise, shifting the PDF as shown. With a finite number of cases, the detectability of such a change in the PDF depends on the ratio of the shift in the mean (signal) to the standard deviation (noise). By increasing the averaging period, say by predicting seasonal mean temperatures rather than daily temperatures, one can increase the signal-to-noise ratio to acceptable levels at the expense of losing the ability to identify individual weather events. In most cases, the standard deviation of daily, or even weekly, averages of extratropical meteorological variables is so large as to make attribution on this timescale impossible by purely statistical methods.

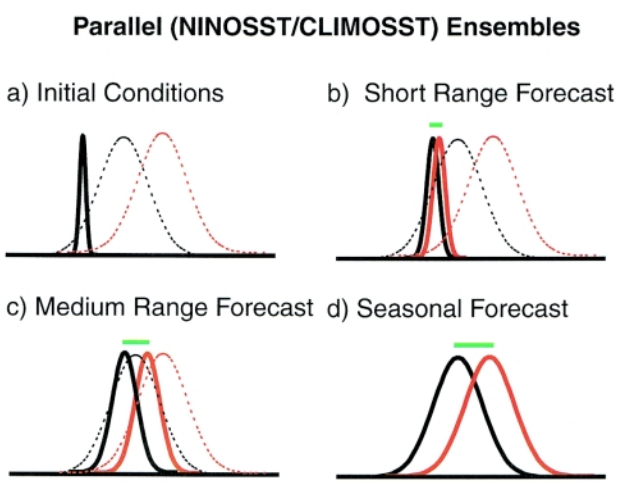

FIG. 9. Schematic PDFs for (a) model initialization, (b) short-term weather forecasts, (c) medium-range weather forecasts, and (d) long-range or seasonal forecasts. The red curves represent the NINOSST ensemble and the black curves the CLIMOSST ensemble. In (a)–(c) the dotted lines reproduce the long-term or seasonal forecast PDFs from (d).

In comparison, the ensemble forecasting technique uses a numerical weather prediction model to forecast a distribution of values of temperature, precipitation, etc., given that the model's initial conditions lie within a certain range of uncertainty. The red curves in Fig. 9 schematically illustrate the evolution of this forecast PDF throughout the forecast period. In our idealized example, the uncertainty in the initial state of the atmosphere is represented by a narrow PDF centered on the analyzed value. For the NCEP ensemble, the 11 members are designed to efficiently sample the initial (multidimensional) PDF so that the ensemble spread grows rapidly. In the short range, the ensemble mean evolution approximately follows the nonlinear forecast model equations. That is, it approximates a deterministic forecast, and the spread among ensemble members remains small. In the medium range, the ensemble spread is significantly larger. In the long range, the ensemble mean eventually approaches the long-term climatological mean of the model, and the spread of the ensemble saturates at the climatological standard deviation of the model. In other words, after a month or so the model has completely forgotten its initial conditions and the forecast ensemble cannot in practice be distinguished from an ensemble drawn at random from the climatological PDF of the model. The actual climatological PDF is a function of the time of year and evolves during the forecast period. However, we have shown it as stationary in Fig. 9 in order to simplify the illustration.

The method of parallel ensembles combines the above approaches, explicitly diagnosing the effects of both boundary and initial conditions on the forecast. As described in section 2 this method uses two sets of runs starting from the same distribution of initial conditions. As depicted in Fig. 9, the CLIMOSST runs (black curves) evolve into the PDF consistent with climatological SSTs, and the NINOSST runs (red curves) evolve into the PDF consistent with the El Niño SSTs. The synoptic El Niño signal (horizontal green bar) tends to grow with time, eventually evolving into the model's seasonal forecast (the "seasonal El Niño signal"). This example illustrates that our method bridges the gap between weather forecasting and seasonal climate forecasting. Note that from

a seasonal perspective, the primary benefit of our method is diagnostic.

b. Signal, skill, and spread

Our experimental design results in a competition among signal, spread, and skill. The seasonal mean rms values of signal, spread, and forecast skill (anomaly correlation) over the Pacific–North America region (60°W–180°, 20°–70°N) are shown in Fig. 10 as a function of forecast lead time. We are counting on the signal outrunning the spread (scaled by the square root of the ensemble size) for our experiments to be statistically significant. The dropoff in forecast skill with forecast lead time results both from model deficiencies and the inherent unpredictability of the atmosphere. To make conclusions about individual weather events in nature *we rely on the El Niño signal becoming large while the model is still skillful.* This typically allows us a "window of opportunity" during which attribution is possible.

It should be no surprise that specifying observed tropical SST anomalies improves medium-range forecast skill in midlatitudes (e.g., see the early study of Rowntree 1972). In the present study, this effect is quantified with a large sample (11 runs for each of 61 cases) over an entire winter season with NCEP's operational ensemble forecast system. Figure 10 shows the anomaly correlation skill over North America for the NINOSST and CLIMOSST ensembles as a function of forecast lead time. The effect on forecast skill appears by day 5 and is sizable during the second week of the forecast. Additionally, the case studies shown above demonstrate that El Niño SSTs can have an impact on rms error over North America of around 5% at 5 days and around 15% at 10 days. Therefore, on average the El Niño signal is physically meaningful.

The question arises whether subseasonal variations in the signal are also meaningful. To test this proposition we stratified the 61 forecasts in our experiment by the rms amplitude of the signal over North America (the same region as used in Fig. 10). The average anomaly correlation skill is 0.62 for the "high signal" (upper tercile) group and 0.44 for the "low signal" (lower tercile) group. The fact that the magnitude of the signal is positively correlated with anomaly correlation skill says that variations in the signal are physically meaningful. This result supports our use of the synoptic El Niño signal to address the attribution problem. However, the forecast anomaly amplitude, which is available from the operational forecasts, is just as good a predictor of AC forecast skill as the

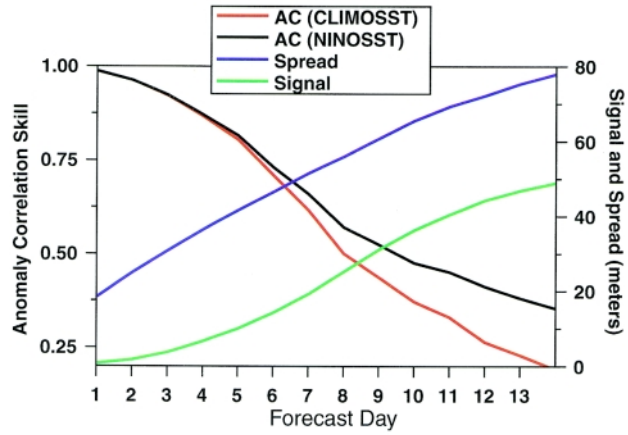

FIG. 10. Anomaly correlation forecast skill for NINOSST and CLIMOSST ensemble means, ensemble spread and root-mean-square signal as a function of forecast lead time. All quantities are calculated using 500-mb height and are averaged over the Pacific–North American region (20°–70°N, 180°–60°W).

El Niño signal. Unfortunately, the CLIMOSST runs have no obvious prognostic value that would be of use to the forecaster in real time.

c. Attribution

The statistical and dynamical issues underlying the question of attribution are subtle. For example, the specific weather on any given day during the 1997/98 winter would almost certainly have been different if there had been no El Niño. But it would also have been different, at least theoretically, had Lorenz's proverbial butterfly flapped its wings a little harder several months prior. In contrast, this study is concerned with how El Niño *systematically* (i.e., in the ensemble mean) changes identifiable storms and circulation patterns. Because of the need to follow identifiable (i.e., forecastable) features, attribution by our method is limited to the effects of El Niño during the forecast period.

In theory, we choose a strict definition of attribution: an observation can be attributed (at least in part) to El Niño if the observed value was more likely to have come from the NINOSST distribution than the CLIMOSST distribution *if it had been drawn at random.* This likelihood is determined by the ratio of the two probability densities evaluated at the observed value. The degree of likelihood needed for attribution is up to the user. Note that attribution may be possible for some variables in some regions and impossible for other variables or other regions. In principle the interpretation is no different for attribution based on seasonal forecasts. However, our method has the potential

to identify the effects of El Niño on subseasonal timescales precisely because ensemble spread of a given variable in the medium range is much smaller than the climatological standard deviation of that variable.

From the above we can derive some practical "rules of thumb" for attribution. First of all, a statistically significant signal is necessary for attribution. A large value of the signal relative to the spread (regardless of sample size) is helpful for attribution, as it results in a greater separation of the PDFs. For the 11-member ensembles used here, the 95% confidence level implies that if the signal is a prominent feature of the verification and the NINOSST forecast, but not the CLIMOSST forecast, then attribution is probable. This is particularly true if the signal is more extreme in the verification than in the operational run so that it lies in a region of relatively little overlap in the PDFs. In such cases a mechanistic explanation for the synoptic El Niño signal will also explain much of what went on in the observations. These rules of thumb were used to attribute important meteorological aspects of the ice storm case and the California rain case to El Niño.

The choice of the meteorological variables and methods used for attribution is ultimately driven by the human impacts of extreme or unusual weather and climate events. These impacts may be due to large damages from individual storms, such as the January 1998 ice storm, or due to damage from a series of storms embedded in a long-wave pattern, as in the case of the California floods of February 1998. These impacts may also be due to the cumulative effects over a season or longer, for example, the reduced heating bills due to the seasonal mean warm anomaly in the northern United States. Seasonal forecasts and climate GCM simulations can address seasonal mean impacts and can also theoretically address the statistical risk of extreme events during a season. Unfortunately, seemingly small errors in the climate of these models can lead to large errors in the model's sensitivity to tropical forcing (Newman and Sardesmukh 1998). It is unclear whether the sensitivities of the climate GCMs on subseasonal timescales are correct. An important benefit of our method is that the simulations stay "close to nature" because they start from observed initial conditions and should, therefore, capture the sensitivities of the atmosphere to tropical forcing on subseasonal timescales. Thus our method provides a new tool to assess the effects of El Niño on individual weather events that actually occurred in nature.

5. Conclusions

We have shown that the method of parallel ensembles of medium-range forecasts with and without SST anomalies is able to diagnose the importance of El Niño for the development of individual large-scale weather events. In some cases we can attribute aspects of a weather event to El Niño and even attempt to quantify that impact. We have also confirmed and quantified the positive effect of tropical SST anomalies on forecast skill in the medium range. Our method gives more information than traditional seasonal forecasts or GCM runs, though both types of simulations are useful in attribution. The choice of method depends on the timescale involved in the human impacts. The set of forecasts for the winter of 1997/98 provides a rich diagnostic resource to study the mechanisms of tropical–extratropical interaction on subseasonal timescales. Though we touched on these only lightly, time-varying Rossby wave propagation and the effect of weekly variations in tropical convection seem to play a role in the cases shown. The effect of anomalous moisture flux on storms also likely plays an important role.

We performed the CLIMOSST runs in near–real time and put our estimate of the synoptic El Niño signal on the World Wide Web. The results for the 1998–99 La Niña are also available. The archive of the Web site is accessible from the CDC home page (http://www.cdc.noaa.gov). The entire dataset will be available to researchers by the end of 1999, though we will accommodate requests for individual cases before then.

Acknowledgments. We thank Mark Borges (CDC), Yuejian Zhu (NCEP), and Mark Iredell (NCEP) for their assistance with the model and in getting the initial conditions. We thank Wes Berg (CDC) for the satellite rainfall products. Discussions with our colleagues, especially C. Penland, are also gratefully acknowledged. Jerry Meehl pointed out the conflicting newspaper headlines. We also thank James Rasmussen for helping to obtain funding for computer resources. This research was partially supported by a grant from the NOAA Office of Global Programs and NSF Grant ATM-9503295.

Appendix: Model testing and validation

The differences in the computers at NCEP (Cray C90) and CDC (Sun E450) introduce three unwanted, but unavoidable, sources of discrepancy between the sets of model runs: coding changes, compiler differences, and machine architecture differences. Postprocessing

of the model output to gridded, pressure level data also introduced small, but unimportant discrepancies. Given these potential sources of error we paid special attention to verifying that the execution of the models on the different machines was similar enough to allow comparison of the two ensembles. Without going into great detail, we reran the NINOSST ensemble at CDC for selected test cases and compared the 500-mb height output with that from NCEP. If the difference between the means of the two ensembles was small compared to the spread of the ensemble, we deemed the model discrepancies to be insignificant, using the significance test described in section 2.

The MRF model underwent significant changes on 7 November 1997, mainly involving code restructuring, and again on 12 January 1998, mainly involving values of the diffusion coefficients. For all forecasts we use the version of the model consistent with that used at NCEP at the time of initialization, with one exception. For the 16 October 1997 case we use the November 1997 version of the model, and we performed both NINOSST and CLIMOSST integrations at CDC. Interestingly, we were able to detect the January change in the NCEP model using the significance test described in section 2 of the paper.

References

Berg, W., W. Olson, R. Ferraro, S. J. Goodman, and F. J. LaFontaine, 1998: An assessment of the first- and second-generation navy operational precipitation retrieval algorithms. *J. Atmos. Sci.,* **55,** 1558–1575.

Ferranti, L., T. N. Palmer, F. Molteni, and E. Klinker, 1990: Tropical–extratropical interaction associated with the 30–60 day oscillation and its impact on medium and extended range prediction. *J. Atmos. Sci.,* **47,** 2177–2199.

Francis, D., and H. Hengeveld, 1998: *Extreme Weather and Climate change.* Atmospheric Environment Service, Environment Canada, 31 pp.

Horel, J. D., and J. M. Wallace, 1981: Planetary-scale atmospheric phenomena associated with the Southern Oscillation. *Mon. Wea. Rev.,* **109,** 813–829.

Kalnay, E., and Coauthors, 1996: The NCEP/NCAR 40-Year Reanalysis Project. *Bull. Amer. Meteor. Soc.,* **77,** 437–471.

Kanamitsu, M., and Coauthors, 1991: Recent changes implemented into the global forecast system at NMC. *Wea. Forecasting,* **6,** 425–435.

Livezey, R. E., M. Masutani, A. Leetma, H. Rui, M. Ji, and A. Kumar, 1997: Teleconnective response of the Pacific–North American region atmosphere to large central equatorial Pacific SST anomalies. *J. Climate,* **10,** 1787–1820.

Newman, M., and P. D. Sardeshmukh, 1998: The impact of the annual cycle on the North Pacific/North American response to remote low-frequency forcing. *J. Atmos. Sci.,* **55,** 1336–1353.

Rowntree, P. R., 1972: The influence of tropical east Pacific Ocean temperatures on the atmosphere. *Quart. J. Roy. Meteor. Soc.,* **98,** 290–321.

Toth, Z., and E. Kalnay, 1993: Ensemble forecasting at NMC: The generation of perturbations. *Bull. Amer. Meteor. Soc.,* **74,** 2317–2330.

——, and ——, 1997: Ensemble forecasting at NCEP and the breeding method. *Mon. Wea. Rev.,* **125,** 3297–3319.